JOURNAL OF AIRCRAFT
Vol. 36, No. 1, January–February 1999

Reduced-Order Models for Integrated Aeroservoelastic Optimization

Moti Karpel*
Technion—Israel Institute of Technology, Technion City, 32000, Haifa, Israel

Recent developments of modal-based aeroservoelastic modeling techniques extended the applicability of the modal approach to almost all of the aeroservoelasticity related aspects of aircraft structural and control design. The various techniques are reviewed and combined for an integrated design optimization scheme, where stress, static-aeroelastic, closed-loop flutter, control margins, time response, and continuous gust constraints are treated with a common basic model. The structure is represented in the basic model by a set of low-frequency normal modes of a baseline design. Design changes are adequately addressed without changing the generalized coordinates. Typical difficulties of the modal approach are alleviated by various optional fictitious-mass and modal-perturbation techniques. Static modes can be added during the optimization process for better convergence to the optimal solution. Minimum-state rational approximation of the unsteady aerodynamics leads to an efficient state-space model that can be augmented by any combination of linear-control components. A physical weighting algorithm is used to improve the aerodynamic approximations and to select modes for truncation or residualization. The reduced-size models and the associated analytic sensitivities to design changes facilitate extremely efficient and adequately accurate on-line optimization sessions.

Nomenclature

$[A]$	= steady generalized aerodynamic force coefficient matrix
$[A_0]$, $[A_1]$, $[A_2]$	= aerodynamic approximation matrices, Eq. (18)
b	= semichord
$\lvert[C_s(ik_l)]^{-1}\rvert$	= matrix of absolute values of the respective terms in $[C_s(ik_l)]^{-1}$
$[C_s(s)]$	= dynamic matrix defined in Eq. (17)
$[D]$, $[E]$	= aerodynamic approximation matrices, Eq. (18)
$[G_c]$	= control gain matrix
$[G_{ka}]$	= aerostructure spline matrix
$[I]$	= unit matrix
$[K]$	= stiffness matrix
k	= reduced frequency, $\omega b/V$
k_l	= tabulated reduced frequency
$\{\boldsymbol{L}\}$	= section loads vector
$[M]$	= mass matrix
n_a	= number of aerodynamic states
n_{dv}	= number of design variables
n_h, n_c, n_g	= number of structural, control, and gust modes
n_L	= number of aerodynamic approximation roots
n_r	= number of rigid-body modes
p_{s_k}	= change in kth structural design variable
$[Q]$	= unsteady generalized aerodynamic force coefficient matrix
$[\tilde{Q}]$	= approximated unsteady aerodynamic matrix
q	= dynamic pressure
q_d	= design dynamic pressure
$[R]$	= aerodynamic approximation root matrix, Eq. (18)
s	= Laplace variable
$[SU]$	= stress/strain coefficient matrix, Eq. (11)
$[T(i\omega)]$	= matrix of transfer functions, Eq. (34)
t	= time
$\{\boldsymbol{u}\}$	= aeroservoelastic input vector, Eq. (24)
V	= true velocity
$[W]$	= least-squares weight matrix
$\bar{W}_{ijl}$	= normalized least-squares weight in Eq. (31)
w	= white-noise input
w_g	= gust velocity
$\{\boldsymbol{x}\}$	= aeroservoelastic state vector, Eq. (24)
$\{\boldsymbol{x}_a\}$, $\{\boldsymbol{x}_c\}$, $\{\boldsymbol{x}_g\}$	= aerodynamic, control, and gust states
$\{\boldsymbol{x}_1\}$, $\{\boldsymbol{x}_2\}$	= retained and eliminated state partitions
$\{\boldsymbol{y}\}$	= aeroservoelastic output vector, Eq. (24)
$\{\boldsymbol{y}_s\}$, $\{\boldsymbol{y}_c\}$	= structural and control outputs
γ_l	= aerodynamic approximation root, Eq. (29)
$\{\Delta\boldsymbol{u}_l^{(1)}\}$	= incremental forces resulting from stiffness changes
$\{\boldsymbol{\delta}\}$	= vector of trim variables
ε_l	= total approximation error, Eq. (31)
$[\lambda]$	= diagonal matrix of eigenvalues
$\{\boldsymbol{\xi}\}$	= structural modal displacements
$\{\boldsymbol{\sigma}\}$	= vector of stresses and strains
Φ	= power spectral density
$[\phi]$	= matrix of vibration modes
$\{\psi_f\}$	= eigenvectors in Eq. (6)
$[\psi_{l_s}]$	= static mode in Eq. (16)
ω	= frequency of oscillations

Subscripts

a	= discrete structural analysis coordinates
ac_i	= related to the ith actuator
b	= related to the baseline structure
c	= related to control modes
e	= related to elastic modes
f	= calculated with fictitious masses
g	= related to gust modes
h	= related to structural modal coordinates
k	= related to aerodynamic grid points, or matrix derivative with respect to p_{s_k}
L	= related to load modes

Received Feb. 24, 1998; revision received May 13, 1998; accepted for publication June 15, 1998.

*Associate Professor. Senior Member AIAA.

r = related to rigid-body modes
s = related to sensor locations
w = related to gust velocity
z = related to gust response point
δ = related to trim variables

Introduction

AEROSERVOELASTICITY deals with the interaction of aircraft structural, aerodynamic, and control systems. The interaction affects the aircraft performance, structural integrity, handling qualities, and growth potential. The increasing demand for high-performance airplanes at affordable cost motivated the development of automated design optimization schemes that can deal with all of the aeroservoelastic design requirements in an integrated manner.[1,2] The modeling methodology has a critical impact on the usefulness of the optimization scheme in realistic design cases. The considerations in the development of a design-modeling methodology should include 1) applicability to the various aeroservoelastic disciplines, 2) typical design scenarios throughout the aircraft development process, 3) required levels of accuracy, 4) compatibility with other analysis and synthesis codes, 5) modeling cost and generation time, 6) efficiency in repetitive analysis, 7) availability of constraint sensitivity to design changes, and 8) user friendliness.

The aeroservoelastic design issues are static and dynamic design loads, associated stress and strain levels, aerodynamic stability derivatives, vibration levels, aeroelastic stability (divergence and flutter), control stability robustness, and continuous gust response. The common approach to the formulation of dynamic aeroelastic equations[3,4] is the modal approach where the structural displacements are represented by a limited set of low-frequency natural vibration modes. Commonly used structural analysis and optimization schemes such as ASTROS[5] and NASTRAN[6] use the modal approach in the dynamic response and stability disciplines, but the static aeroelastic and stress disciplines are treated by the discrete approach with typically large-order finite element models with thousands of degrees of freedom. The computational costs associated with the repeated construction of the full discrete finite element models and the large-order analysis degrade the usefulness of the optimization scheme, particularly in the preliminary design stages when extensive tradeoff studies for various design concepts are needed.

Some techniques were developed to reduce the optimization model size. Reference 7 used the equivalent plate approach,[8] which requires special modeling efforts and might not correspond to actual structures as well as standard finite element models. It may provide, however, valuable information for preliminary design with significantly lower model construction efforts and computational cost. Reference 9 used the perturbation-mode approach,[10] in which the displacements resulting from each loading case are linear combinations of the baseline displacement vector and its derivatives with respect to the design variables. The problem size in this case is equal to the number of global design variables plus one. The application of Ref. 9 showed efficient and accurate solution in optimization with one design-load case. This approach, however, does not take into account load redistributions caused by structural changes, and may become inefficient in optimization with multiple loading cases.

Another reduced-order modeling methodology resulted from the extension of the modal approach to the static aeroservoelastic disciplines. The extension started with the aeroelastic control effectiveness[11,12] and static design loads.[13] Further extensions to stress and strain considerations in design maneuver cases required the development of modal perturbation techniques.[14-17] In addition, the modal basis can be expanded during the optimization process by including static modes, following the reanalysis concepts of Refs. 18 and 19. Local effects caused by concentrated loads or large structural changes can be treated by fictitious-mass techniques.[16,20]

The use of fixed-basis modal design models for the dynamic aeroelastic disciplines started long before their usage in the static disciplines.[21] Other than using a fixed basis, the formulation in Ref. 21 was that of a classic frequency-domain flutter analysis with transcendental unsteady aerodynamic force coefficient matrices.[5,6] Some control-system effects can be accommodated by the frequency-domain approach, but the application of various modern control-design techniques[22,23] requires the aeroservoelastic equations of motion to be transformed into a first-order, time-domain (state-space) form. This transformation requires the aerodynamic matrices to be approximated by rational functions in the Laplace domain.[24-28] The resulting aeroelastic state-space model can be augmented by a control model for various aeroservoelastic optimization studies with flutter, control stability margins, and continuous gust constraints.[7,27-29] Some of these techniques are currently being implemented in ASTROS.[30]

Framework of an Optimization Session

The process of developing a new flight vehicle is based on several major design cycles from the early conceptual design, through preliminary, advanced, and final designs, to repeated modifications after the vehicle is already in service. The need for integrated analysis and design exists in all of these cycles, even though the model details, the scope of investigated issues, the required accuracy, and the range of design variables change. Each design cycle starts with baseline linear structural, as well as aerodynamic and control models, which are based on previous design cycles. It is assumed that the structure is modeled by a standard finite element model that is most likely quite coarse at preliminary design stages and more detailed at later stages. The aerodynamic model is used to calculate aerodynamic loads as function of the aircraft trim variables and the elastic deformations. The control model is based on interconnected control elements (sensors, control laws, and actuators), defined by their transfer functions or state-space realizations. The design variables are selected structural gauges and control parameters. While keeping the aerodynamic and structural planform geometry unchanged, the task of a basic optimization session is to find the values of the design variables that minimize the structural weight without violating the aeroservoelastic behavior constraints.

A schematic description of a typical automated design session is given in Fig. 1. The modal database is constructed for a relatively large number of low-frequency vibration modes (about 40), and additional kinematic control-surface deflection modes and sinusoidal gust modes. The database contains all of the ingredients for the various analyses and sensitivity calculations throughout the optimization process. Each iteration starts with combining the database ingredients for a reduced-size aeroservoelastic model, followed by analysis and constraint sensitivity calculations. A constrained function minimization scheme is used at the end of each iteration to progress toward an optimum within prescribed move limits. The formulation was arranged such that the computational cost of generating the database is relatively heavy, but the subsequent model assembly, analysis, and sensitivity computations during the design iterations are extremely efficient. Once a database is constructed, the designer can perform numerous design studies, with various analysis parameters, control filters, design constraints, and move limits with the same database.

Typical modal-based integrated optimization runs, with several of the disciplines of Fig. 1 considered simultaneously, take several minutes on today's workstations.[14-17,28] This facilitates on-line design studies and the integration of the basic optimization scheme into a larger one that evaluates different design concepts with variable airplane geometry. More details on the separation between database construction and design iterations are given in the following sections.

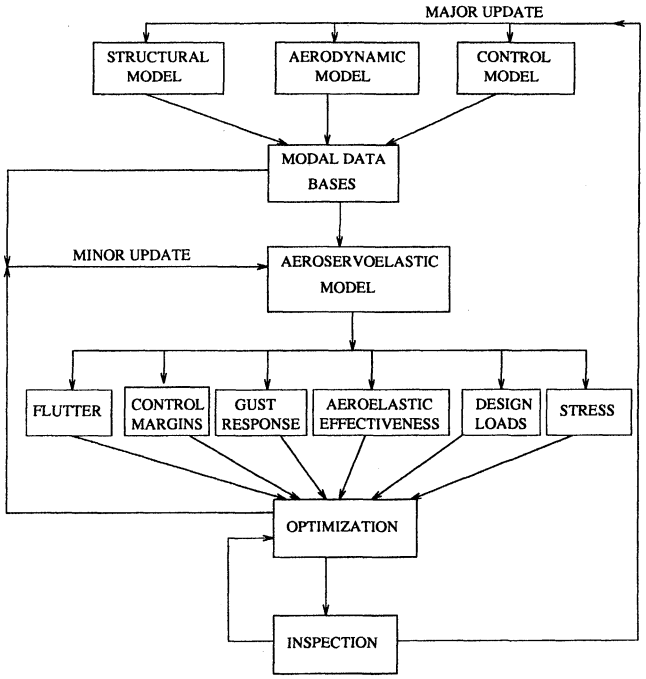

Fig. 1 Scheme of an optimization session.

Basic Modal Approach

The basic assumption of the modal approach in aeroservoelastic problems is that the structural displacements $\{u_a\}$ (static or dynamic) in response to external excitation can be adequately expressed as a linear combination of a relatively small set of displacement modes:

$$\{u_a\} = [\phi_{ar}]\{\xi_r\} + [\phi_{ae}]\{\xi_e\} + [\phi_{ac}]\{\xi_c\} \tag{1}$$

where the vectors $\{\xi\}$ are generalized displacements with the subscripts r, e, and c relate to the structural rigid-body, elastic, and control modes, respectively. The structural modes in our scheme are the n_h lowest frequency normal modes $[\phi_{ah}] = [\phi_{ar}\phi_{ae}]$ of the baseline structure, which satisfy the eigenvalue problem

$$[K_{aa}][\phi_{ah}] = [M_{aa}][\phi_a][\lambda] \tag{2}$$

where $[K_{aa}]$ and $[M_{aa}]$ are the baseline finite element analysis stiffness and mass matrices, respectively, and $[\lambda]$ is a diagonal matrix of the corresponding eigenvalues, $\lambda_i = \omega_i^2$, where ω_i are the n_h lowest natural frequencies including n_r rigid-body ones that equal zero. A convenient way to generate the kinematic control modes $[\phi_{ac}]$ in a standard finite element code is discussed in Ref. 28.

While the structural properties vary during the optimization run, the generalized coordinates remain those of the baseline structure. With the baseline modes normalized to unit generalized masses, the generalized stiffness and mass matrices are updated during the design process by

$$[K_{hh}] = [\lambda] + \sum_{k=1}^{n_{dv}} [K_{hh}]_k p_{s_k} \tag{3}$$

where

$$[K_{hh}]_k = [\phi_{ah}]^T[K_{aa}]_k[\phi_{ah}]$$

$$[M_{hh}\ M_{hc}] = [I\ M_{hc_b}] + \sum_{k=1}^{n_{dv}} [M_{hh}\ M_{hc}]_k p_{s_k} \tag{4}$$

where

$$[M_{hh}\ M_{hc}]_k = [\phi_{ah}]^T[M_{aa}]_k[\phi_{ah}\ \phi_{ac}]$$

where p_{s_k} is the deviation of the kth structural design variable from its baseline value, and $[K_{aa}]_k$ and $[M_{aa}]_k$ are the derivatives of the discrete structural matrices with respect to the structural design variables. The coefficient matrices in Eqs. (3) and (4) are extracted from the finite element model and are stored in the database.

Generation of Baseline Modes

The solution of Eq. (2) for a set of lowest eigenvalues and the associated eigenvectors of the baseline structure generates the fixed modal basis. The order of complete-aircraft models for stress and aeroelastic analyses is typically 3000–30,000 degrees of freedom. Adequate solutions for this problem size are standard features of common finite element codes.[5,31]

There are several ways to affect the baseline modes to improve their performance as fixed generalized coordinates throughout the optimization run. The obvious way is to increase their number, which, of course, adversely affects the numerical efficiency in subsequent analyses. The number of 30–40 modes was shown in several studies[12–17,28] to be adequate in realistic aeroelastic optimization studies. This relatively high number of modes is required mainly for stress and static aeroelastic constraints.

Another way to affect the baseline modes is by using the Guyan's static condensation.[31] While in the regular discrete-coordinate approach, static condensation is just a numerical option with no effect on the static results, it does affect modal-based results through its effects on the modes taken into account. In many cases the condensation is not effective and might even increase the modal-based errors.[17] However, when applied to structural parts that are not subject to redesign, the condensation was shown in Ref. 17 to yield accurate results and cause a significant reduction in computation time. The formulation required to support the static condensation option (when modal-based optimization is integrated in a standard finite element code) is also given in Ref. 17.

A major disadvantage of the modal approach is in its inaccuracy in predicting local response to concentrated loads. This difficulty can be cured by adding large fictitious masses at the points of force application when the baseline modes are calculated.[16,20] The eigenproblem of Eq. (2) is replaced by

$$[K_{aa}][\phi_f] = [M_{aa} + M_f][\phi_f][\lambda_f] \tag{5}$$

where $[M_f]$ is a matrix of the added fictitious masses in desired locations. This is solved for the n_h eigenvalues $[\lambda_f]$ and eigenvectors $[\phi_f]$. The structural displacements are now expressed as linear combinations of the new modes $[\phi_f]$, and reduced-order models for the original structure (without fictitious masses) are obtained when the fictitious masses are removed, the $n_h \times n_h$ eigenproblem

$$[\lambda_f][\psi_f] = [I - \phi_f^T M_f \phi_f][\psi_f][\lambda] \tag{6}$$

is solved for the n_h eigenvalues $[\lambda]$ and the square eigenvector matrix $[\psi_f]$. The baseline modes are then calculated by

$$[\phi_{ah}] = [\phi_f][\psi_f] \tag{7}$$

The low eigenvalues in $[\lambda]$, and the associated modes in $[\phi_{ah}]$ are typically almost identical to those of the nominal finite-element model. The highest-frequency modes reflect local deformations and are not necessarily actual *physical* natural modes. They are requested, however, to account for local deformations in subsequent analyses. The use of fictitious masses is extremely effective in cases where most of the external loads are fairly well distributed (such as in aerodynamic loading),

but a few specific points are loaded by large concentrated forces (such as in store release[32] or actuator application[33] cases). Fictitious masses can also be used to facilitate modal coupling in repeated analysis with many store configurations,[34] and to allow large local structural changes without changing the modal basis.[35]

Static Aeroelastic Considerations

Static aeroelasticity deals with quasisteady aircraft maneuvers where elastic deformations caused by a disturbance, and the associated changes in aerodynamic loads and rigid-body accelerations can be assumed to reach static equilibrium immediately. While this assumption is usually adequate for maneuver and divergence analyses, the full dynamic equations (see later sections) may have to be considered when the vibration roots are close to the rigid-body stability roots, as happens when the aircraft is very large or flexible, or when unique configurations such as the forward-swept wing are involved. The basic assumption implies that the elastic deformations are orthogonal to the rigid-body modes. While the classic discrete-coordinate approach[36] needed a series of operations to implement this condition, the basic modal approach got it automatically because of the orthogonality of free–free elastic modes to the rigid-body ones.[11] Mathematically, the basic assumption implies that the effects of the elastic velocities and accelerations, $\{\dot{\xi}_e\}$ and $\{\ddot{\xi}_e\}$, on the static aeroelastic equilibrium are negligible.

Linear static aeroelastic codes are commonly based on aerodynamic panel methods that produce Mach-dependent force coefficient matrices that relate aerodynamic loads on the panels to local angles of attack. Pre- and postmultiplications of the panel matrices by modal deflections and slopes, transformed to the aerodynamic grid by spline techniques, generate the steady aerodynamic force coefficient matrix $[A_{hh}]$. The splined modes can also be used to generate the generalized force coefficient matrix $[A_{h\delta}]$, where the subscript δ relates to the vector $\{\delta\}$ of trim variables such as angle of attack, control surface deflection, and roll rate.

The formulation and solution of static–aeroelastic equilibrium equations in modal coordinates were presented in Refs. 15 and 16. A general form of the equilibrium equation is

$$\begin{bmatrix} -qA_{rr} & -qA_{re} & M_{rr} \\ -qA_{er} & K_{ee} - qA_{ee} & M_{er} \\ M_{rr} & M_{er}^T & 0 \end{bmatrix} \begin{Bmatrix} \xi_r \\ \xi_e \\ \ddot{\xi}_r \end{Bmatrix} = \begin{bmatrix} qA_{r\delta} \\ qA_{e\delta} \\ 0 \end{bmatrix} \tag{8}$$

The last row in Eq. (8) relates rigid-body displacements to the elastic ones. For the baseline structure $[M_{er}] = 0$ and, hence, $\{\xi_r\} = 0$. However, when the structure changes, a nonzero $\{\xi_r\}$ is needed to enforce orthogonality between the elastic deformations and the rigid-body modes.[15] Equation (8) yields the trim equation

$$[M_{rr}]\{\ddot{\xi}_r\} = q[\tilde{A}_{r\delta}]\{\delta\} \tag{9}$$

where

$$[\tilde{A}_{r\delta}] = ([I] + q[\bar{A}_{re}][\bar{K}_{ee}]^{-1}[M_{er}][M_{rr}]^{-1})^{-1} \times ([A_{r\delta}] + q[\bar{A}_{re}][\bar{K}_{ee}]^{-1}[A_{e\delta}])$$

where

$$[\bar{K}_{ee}] = [K_{ee}] - q([A_{ee}] - [A_{er}][M_{rr}]^{-1}[M_{er}]^T]$$

$$[\bar{A}_{re}] = [A_{re}] - [A_{rr}][M_{rr}]^{-1}[M_{er}]^T$$

The flex-to-rigid ratios between terms in $[\tilde{A}_{r\delta}]$ and $[A_{r\delta}]$ define the aeroelastic effectiveness parameters that can be used as optimization constraints. The aeroelastic effectiveness of other aerodynamic coefficients, such as a hinge moment resulting from trim variables in $[A_{c\delta}]$, can also be calculated in a similar way. Hinge-moment constraints may play an important role in cases where the maneuvers are limited by hydraulic force saturation.[12] Divergence occurs when $[\bar{K}_{ee}]$ of Eq. (9) becomes singular. This is a structural divergence where (under the basic assumptions) the structure breaks before rigid-body motion starts. Aerodynamic divergence that involves rigid-body motion is discussed later.

The solution of Eq. (9) for the n_r free trim variables and the recovery of $\{\xi_r\}$ and $\{\xi_e\}$ by Eq. (8) facilitates the calculation of the net loads

$$\{P_a\} = q[G_{ka}]^T([A_{k\delta}]\{\delta\} + [A_{kr}]\{\xi_r\} + [A_{ke}]\{\xi_e\}) - [M_{aa}][\phi_{ar}]\{\ddot{\xi}_r\} \tag{10}$$

where the aerodynamic matrices contain panel load coefficients because of trim parameters and $[G_{ka}]$ is the structure-to-aero spline matrix.

It can be observed that the trim variables, net loads, and effectiveness constraints are functions of the design variables. The differentiation of Eqs. (8–10) with respect to the design variables results in analytical sensitivity expressions.[15] The order of Eq. (8) is typically two to three orders of magnitude smaller than the equivalent one in common discrete-coordinate schemes, which facilitates huge computation time savings in modal-based optimization with static aeroelastic considerations. The accuracy of the modal approach has been shown to be very high in several realistic static–aeroelastic design studies.[12,14–17]

Stress and Strain Considerations

Element stresses and strains can be related to the structural displacements by

$$\{\sigma\} = [SU]\{u_l\} \tag{11}$$

where $[SU]$ is a fixed matrix, and $\{u_l\}$ is a subset of $\{u_a\}$, obtained after clamping n_r selected degrees of freedom to eliminate rigid-body displacements. It was shown in Ref. 14 that the use of Eq. (1) with a small number of modes to calculate the displacement vector is fairly adequate for stress analysis only with the baseline structure. The use of the basic modal approximation of Eq. (1) might be grossly inaccurate for stress analysis with structural modifications. The most accurate way to perform stress/strain analysis is by updating the full finite element stiffness matrix and solving for displacements under the updated loads of Eq. (10), as done in Ref. 13. This hybrid approach is easy to implement when the modal and discrete schemes are integrated in one code.[16] It might be very inefficient, however, with large models, or in computation schemes in which the modal database is generated by a discrete scheme and then exported for optimization with a separate modal-based scheme, as done in Ref. 14.

Reference 14 modified the basic modal approach by supplementing the modal database with modal perturbations. The displacement vector for stress analysis of the modified structure is expressed as

$$\{u_l\} = \{u_l\}_b + \{\Delta u_l^{(1)}\} \tag{12}$$

where $\{u_l\}_b$ is the elastic displacement of the baseline structure under the modified net loads, and $\{\Delta u_l^{(1)}\}$ is the incremental

displacement change caused by forces applied by the added material on the baseline structure. The subscript l in the following formulation indicates $\{u_l\}$-related matrix partitions. The first term of Eq. (12) can be formulated by the mode-displacement (MD) approach as[14]

$$\{u_l\}_{b_{MD}} = [\phi_{le}]\left([I] + [\lambda]^{-1}\left[\sum_{k=1}^{n_{dv}} p_{s_k}[K_{ee}]_k\right]\right)\{\xi_e\} \quad (13)$$

Alternatively, when the discrete and modal-based codes are integrated, it is more effective to use the summation-of-force (SOF) approach using the already decomposed baseline stiffness matrix to calculate

$$\{u_l\}_{b_{SOF}} = [K_{ll}]^{-1}\{P_l\} \quad (14)$$

The second term in Eq. (12) is

$$\{\Delta u_l^{(1)}\} = -[K_{ll}]^{-1}\left[\sum_{k=1}^{n_{dv}} p_{s_k}[K_{ll}]_k[\phi_{le}]\right]\{\xi_e\} \quad (15)$$

where the products $[K_{ll}]_k[\phi_{le}]$ are modal force perturbations that can be stored in the database before the optimization starts.[15] When the optimization is performed in a separate code, it is more efficient to premultiply the modal perturbations by $[SU][K_{ll}]^{-1}$ [see Eq. (11)] during the finite element run and store them in the database as modal stress perturbations.[14] Analytical expressions for the sensitivity of stress constraints in design maneuver load cases, which take into account loads redistribution effects, are given in Refs. 14 and 15. The formulation necessary for using static condensation in conjunction with modal-based stresses is given in Ref. 17.

Reference 15 describes implementation of the modal-based static aeroelastic and stress formulation in ASTROS and application to design cases with 3761 and 26,259 structural degrees of freedom. It was shown that the total CPU time required for modal analysis and the construction of a database for modal-based optimization was similar to that required for a single discrete analysis. It was also shown that modal-based design iterations were between one and two orders of magnitudes faster than the discrete-coordinate ones. A design iteration includes a detailed analysis, sensitivity analysis, and an approximate optimization within the user-defined move limits, and under the assumption that the gradients are not functions of the design values. With the modal database already constructed, a modal-based design iteration in the 3761 degree-of-freedom case took 24 s on an Indigo 2 SGI workstation, which implies that realistic design studies can be performed in an on-line manner. Modal results were in excellent agreement with the discrete ones for all of the analyzed cases. Comparisons were also good at the end of optimization cycles with considerable design changes. However, it was indicated that as the structure is being changed, the stress errors associated with the modal approach might grow beyond acceptable levels. It was recommended to update the modal database when design variables are changed by more than 10%.

To allow larger move limits between database updates, Ref. 16 used the first-order displacement approximation of Eq. (12) to calculate higher-order approximations in an iterative process. It improved the accuracy of the resulting stresses, but somewhat slowed down the modal-based process. A more cost-effective approach is to expand the modal basis to include the local deformations calculated by Eq. (15) in a previous iteration. A scheme for supplementing the modal basis by new static modes $\{\phi_{ls}\}$ in each iteration, is presented in Ref. 37. The new mode is based on the incremental displacement vector $\{\Delta u_l^{(1)}\}$ of Eq. (15) as calculated at the end of the previous iteration, orthogonalized with respect to the current modal coordinates such that the resulting $\{\phi_{ls}\}$ satisfies

$$[\phi_{le}]^T[K_{ll}]_b\{\phi_{ls}\} = \{0\} \quad (16)$$

Even though different static modes are added for different maneuver design cases, the expansion of the database is very effective and improves the accuracy of both static aeroelastic and stress constraints for a moderate computational cost.

State-Space Dynamic Equations of Motion

The Laplace transform of the open-loop dynamic aeroelastic equation of motion in generalized coordinates, excited by control-surface motion and atmospheric gusts, is

$$[C_s(s)]\{\xi_h(s)\} = -([M_{hc}]s^2 + q[Q_{hc}(s)])\{\xi_c(s)\} - (q/V)\{Q_{hg}(s)\}w_g(s) \quad (17)$$

where

$$[C_s(s)] = [M_{hh}]s^2 + [B_{hh}]s + [K_{hh}] + q[Q_{hh}(s)]$$

where $\{\xi_h\}$ is the vector of generalized structural displacements, $\{\xi_c\}$ is the vector of control-surface commanded deflections (namely the actuator outputs), w_g is the gust velocity, and $[Q_{hh}]$, $[Q_{hc}]$, and $\{Q_{hg}\}$ are the generalized unsteady aerodynamic force coefficient (AFC) matrices associated with the structural, control, and gust modes. The generalized matrices $[K_{hh}]$, $[M_{hh}]$, and $[M_{hc}]$ are defined in Eqs. (3) and (4). The generalized damping matrix $[B_{hh}]$ is usually a constant matrix based on estimated modal damping values. Specific discrete-coordinate damping terms can be treated similarly to the stiffness terms in Eq. (3).

The main difficulty in constructing and solving Eq. (17) is that the AFC matrices are normally not available as an explicit function of s. Common unsteady aerodynamic routines assume that the structure undergoes harmonic oscillations and generate the complex AFC matrices (at a given Mach number) for various values of tabulated reduced frequency $k = \omega b/V$, where b is a reference semichord. Frequency domain methods are then used for dynamic response and stability analysis with the AFC matrices interpolated from the tabulated ones. The integrated design models used in this work are based on state-space, time-domain, constant coefficient equations, which requires the AFC matrices to be expressed as rational functions of s.

Reference 38 showed that any rational function approximation of $[Q(s)] = [Q_{hh}Q_{hc}Q_{hg}]$ that leads to a state-space aeroelastic model can be cast in the form

$$[\tilde{Q}(p)] = [A_0] + [A_1]p + [A_2]p^2 + [D]([I]p - [R])^{-1}[E]p \quad (18)$$

where p is the nondimensional complex Laplace variable $p = sb/V$ and all of the matrix coefficients are real valued. The $[A_i]$ and $[E]$ matrices in Eq. (4) are column partitioned as

$$[A_i] = [A_{h_i}\ A_{c_i}\ A_{g_i}] \quad (i = 0, 1, 2), \qquad [E] = [E_h\ E_c\ E_g] \quad (19)$$

The gust-related column of $[A_2]$ in Eq. (4) is usually set to $\{A_{g2}\} = 0$ to avoid the unnecessary $\dot{w}_g$ terms in the time-domain model. The resulting state-space open-loop plant equation of motion is

$$\begin{bmatrix} I & 0 & 0 \\ 0 & -\bar{M}_h & 0 \\ 0 & 0 & I \end{bmatrix}\begin{Bmatrix} \dot{\xi}_h \\ \ddot{\xi}_h \\ \dot{x}_a \end{Bmatrix} = \begin{bmatrix} 0 & I & 0 \\ \bar{K}_h & \bar{B}_h & \bar{D} \\ 0 & E_h & \bar{R} \end{bmatrix}\begin{Bmatrix} \xi_h \\ \dot{\xi}_h \\ x_a \end{Bmatrix} + \begin{bmatrix} 0 & 0 & 0 \\ \bar{K}_c & \bar{B}_c & \bar{M}_c \\ 0 & E_c & 0 \end{bmatrix}\begin{Bmatrix} \xi_c \\ \dot{\xi}_c \\ \ddot{\xi}_c \end{Bmatrix} + \begin{bmatrix} 0 & 0 \\ \bar{K}_g & \bar{B}_g \\ 0 & \bar{E}_g \end{bmatrix}\begin{Bmatrix} w_g \\ \dot{w}_g \end{Bmatrix} \quad (20)$$

where

$$[\bar{M}_h] = [M_{hh}] + (qb^2/V^2)[A_{h_2}], \qquad [\bar{K}_h] = [K_{hh}] + q[A_{h_0}]$$
$$[\bar{B}_h] = [B_{hh}] + (qb/V)[A_{h_1}], \qquad [\bar{M}_c] = [M_{hc}] + (qb^2/V^2)[A_{c_2}]$$
$$[\bar{K}_c] = q[A_{c_0}], \qquad [\bar{B}_c] = (qb/V)[A_{c_1}], \qquad [\bar{D}] = q[D]$$
$$[\bar{R}] = (V/b)[R], \qquad \{\bar{\boldsymbol{K}}_g\} = q\{\boldsymbol{A}_{g_0}\}$$
$$\{\bar{\boldsymbol{B}}_g\} = (qb/V)\{\boldsymbol{A}_{g_1}\}, \qquad \{\bar{\boldsymbol{E}}_g\} = (1/V)\{\boldsymbol{E}_g\}$$

The resulting number of aerodynamic augmenting states in $\{\boldsymbol{x}_a\}$ is the order (n_a) of the aerodynamic lag matrix $[R]$.

It is assumed in this work that the control system, including the actuator dynamics, can be expressed in a state-space form as

$$\{\dot{\boldsymbol{x}}_c\} = [A_c]\{\boldsymbol{x}_c\} + [B_c]\{\boldsymbol{u}\}$$
$$\{\boldsymbol{y}_c\} = [C_c]\{\boldsymbol{x}_c\} + [D_c]\{\boldsymbol{u}\} \tag{21}$$

where $\{\boldsymbol{y}_c\}$ includes two types of control outputs: 1) control-surface motion states $\{\boldsymbol{\xi}_c\}$, $\{\dot{\boldsymbol{\xi}}_c\}$, and $\{\ddot{\boldsymbol{\xi}}_c\}$, and 2) other outputs needed for control system analysis. The $[D_c]$ rows associated with the control-surface motion states are zero because the actuators are modeled in our scheme by the third-order transfer function

$$\frac{\xi_{c_i}(s)}{u_{ac_i}(s)} = \frac{a_{i3}}{s^3 + a_{i1}s^2 + a_{i2}s + a_{i3}} \tag{22}$$

where u_{ac_i} is the commanded (input) control surface deflection. Higher-order actuator dynamics can be defined by connecting additional transfer functions in series to u_{ac_i} as part of the control-system model discussed in detail in a separate section.

It is also assumed that a gust filter can be defined in the state-space form

$$\{\dot{\boldsymbol{x}}_g\} = [A_g]\{\boldsymbol{x}_g\} + \{\boldsymbol{B}_g\}w$$
$$\{\boldsymbol{y}_g\} = [C_g]\{\boldsymbol{x}_g\} \tag{23}$$

where $\{\boldsymbol{y}_g\}^T = [w_g \dot{w}_g]$ such that the power spectral density function of the gust velocity w_g is obtained when w represents a white-noise process.

Equations (20–23) combine for the open-loop aeroservoelastic state-space equation

$$[Z]\{\dot{\boldsymbol{x}}\} = [A]\{\boldsymbol{x}\} + [B]\{\boldsymbol{u}\} + \{\boldsymbol{B}_w\}w$$
$$\{\boldsymbol{y}\} = [C]\{\boldsymbol{x}\} + [D]\{\boldsymbol{u}\} \tag{24}$$

where

$$\{\boldsymbol{x}\} = \begin{Bmatrix} \boldsymbol{\xi}_h \\ \dot{\boldsymbol{\xi}}_h \\ \boldsymbol{x}_a \\ \boldsymbol{x}_c \\ \boldsymbol{x}_g \end{Bmatrix}, \quad [B] = \begin{bmatrix} 0 \\ 0 \\ 0 \\ B_c \\ 0 \end{bmatrix}, \quad \{\boldsymbol{B}_w\} = \begin{Bmatrix} 0 \\ 0 \\ 0 \\ 0 \\ \boldsymbol{B}_g \end{Bmatrix}, \quad \{\boldsymbol{y}\} = \begin{Bmatrix} \boldsymbol{y}_s \\ \boldsymbol{y}_c \end{Bmatrix}$$

where $\{\boldsymbol{y}_s\}$ may include structural displacements, velocities, accelerations, and element stresses, and $\{\boldsymbol{y}_c\}$ is the control output of Eq. (21). Structural motion parameters are related directly to $\{\boldsymbol{\xi}_h\}$, $\{\dot{\boldsymbol{\xi}}_h\}$, and $\{\ddot{\boldsymbol{\xi}}_h\}$ via the modal values $[\phi_{sh}]$ at the sensor locations. Structural stresses are related to the subset $\{\boldsymbol{\xi}_e\}$ of $\{\boldsymbol{\xi}_h\}$ by the MD version of Eqs. (11–15). In any case, none of the structural outputs is directly related to w or $\{\boldsymbol{u}\}$.

The aeroservoelastic loop is closed by relating the control inputs to system outputs by

$$\{\boldsymbol{u}\} = [G_c]\{\boldsymbol{y}\} \tag{25}$$

The substitution of Eq. (25) into Eq. (24) yields the closed-loop equation of motion

$$[Z]\{\dot{\boldsymbol{x}}\} = [\bar{A}]\{\boldsymbol{x}\} + \{\boldsymbol{B}_w\}w \tag{26}$$

where only the control related row of $[\bar{A}]$ is different than that of $[A]$ in Eq. (24). A control input term $\{\boldsymbol{u}\}$ can be left in the right side of Eq. (26) to reflect pilot commands in dynamic response analyses.

The control systems of actively controlled vehicles is usually designed in three different stages. The basic system is designed with no, or very little, aeroservoelastic considerations. Modifications are then performed for a family of aeroelastic plant models given in the form of Eq. (20). The modified system, which is normally a function of the flight conditions, is then included in the model of Eq. (24) for an integrated design process. The control model can be defined at this stage by Eqs. (23) and (25) such that the control design variables appear as gain terms in $[G_c]$. In this way, the differentiation of the system matrices of Eqs. (24) and (26) with respect to the control design variables p_{c_k} is straightforward. Other nonzero terms in $[G_c]$ are those with respect to which control stability margins are to be defined in terms of gain and phase margins and singular values.[29,39]

Because the aerodynamic planform shape and the generalized coordinates are fixed throughout the basic optimization process, the derivatives of the system matrices with respect to the structural design variables p_{s_k} are very simple expressions. The only portions of $[Z]$ and $[A]$ that depend on p_{s_k} are the generalized structural matrices of Eqs. (3) and (4). The output matrix $[C]$ depends on p_{s_k} only in cases of acceleration or stress feedback.

The order of the aeroservoelastic state-space model is a function of the number of aerodynamic approximation roots, the number of selected modes, the order of the control system (including sensors, control laws, and actuators), and the gust filters. Important aspects of these issues are discussed in the following sections.

Rational Function Approximations

Various techniques for rational function approximations of the AFC matrices were reviewed in Refs. 25 and 40. Most methods are variations of either the least-square method of Roger[24] or the minimum-state (MS) method.[38] All of the techniques use the frequency-domain-tabulated AFC data to generate a least-square approximation of the coefficient matrices in Eq. (18) with the nondimensional Laplace variable p replaced with ik. Separation into real and imaginary parts leads to

$$\mathrm{Re}[\tilde{Q}(ik)] \equiv [\tilde{F}(k)] = [A_0] - k^2[A_2] + k^2[D](k^2[I] + [R]^2)^{-1}[E] \tag{27}$$

and

$$\mathrm{Im}[\tilde{Q}(ik)] \equiv [\tilde{G}(k)] = k[A_1] - k[D](k^2[I] + [R]^2)^{-1}[R][E] \tag{28}$$

The comparison of Eqs. (27) and (28) with the real and imaginary parts, $[F(k_l)]$ and $[G(k_l)]$, of the tabulated AFC matrices $[Q(ik_l)]$ provides an overdetermined set of approximate equations. With the diagonal root matrix $[R]$ defined by the user, the task of the approximation procedure is to find the combination of the coefficient matrices ($[A_i]$, $[D]$, $[E]$) that fits the tabulated data in the least-square sense. The differences between the various approximation methods can be expressed in terms of the approximation formula, constraints, and data weighting.

The original formula of Roger's approximation is

$$[\tilde{Q}(ik)] = [A_0] + ik[A_1] - k^2[A_2] + \sum_{l=1}^{n_L} \frac{ik}{ik + \gamma_l}[A_{l+2}] \tag{29}$$

which can be cast in the form of Eqs. (27) and (28) with

$$[D] = [I \; I \; \cdots], \qquad [R] = -\begin{bmatrix} \gamma_1 I & & \\ & \gamma_2 I & \\ & & \ddots \end{bmatrix}, \qquad [E] = \begin{bmatrix} A_3 \\ A_4 \\ \vdots \end{bmatrix} \tag{30}$$

The matrix coefficients of Eq. (29) are found by solving a separate least-square problem for each term of $[\tilde{Q}]$, with n_L common approximation roots γ_l. The resulting number of aerodynamic states is $n_a = n_L \times n_h$, where n_h is the number of vibration modes. The modified matrix Padé (MMP) method[40] applies Eq. (29) to each column separately in a way that allows the number of lags and their values to be different for different columns, which can lead to a lower number of states. Typical values of n_L in Roger's and MMP applications are 2–4, which implies that the number of aerodynamic states is typically larger than the number of structural states when Roger-type approximations are used.

The MS method added the terms of $[D]$ to those of $[A_0]$, $[A_1]$, $[A_2]$, and $[E]$ as free approximation coefficients, and allowed the diagonal values in $[R]$ to be distinct. The task is to find the free approximation coefficients that minimize, under some constraints, the total least-square approximation error (summation over all i, j terms and all frequencies l)

$$\varepsilon_t = \sqrt{\sum_{i,j,l} |\tilde{Q}_{ij}(ik_l) - Q_{ij}(ik_l)|^2 W_{ijl}^2} \tag{31}$$

where W_{ijl} is the weight assigned to the ijth term of the lth-tabulated AFC matrix. Weights can be used by the analyst to force better fits for selected aerodynamic terms at specified frequencies, or for simply normalizing the tabulated data. A physical weighting algorithm, which assigns weights according to effects on aeroelastic characteristics, is discussed in the following section.

Because $[D]$ and $[E]$ are both unknowns, the least-square problem is nonlinear. The unconstrained iterative solution[26,38] starts with an initial guess of $[D]$. A linear least-square routine is then applied to solve for $[A_0]$, $[A_1]$, $[A_2]$, and $[E]$, column by column. The resulting $[E]$ is then fixed and a least-square problem is solved for $[A_0]$, $[A_1]$, $[A_2]$, and $[D]$, row by row. Such $[D] \rightarrow [E] \rightarrow [D]$ iterations are repeated for a predefined number of iterations or until the error of Eq. (7) is converged. Unless ill-conditioning occurs in the least-square solution, the total error, Eq. (31), is reduced monotonously.

The full development of the approximation process is given in Ref. 41. The number of unknowns in the unconstrained problem is $3n_h + n_a$ in each $[D] \rightarrow [E]$ solution and $3(n_h + n_c + n_g) + n_a$ in each $[E] \rightarrow [D]$ solution. In the current context, *constraints* are conditions in which the approximation is forced to match the tabulated data exactly at some reduced frequencies. The resulting equations are used to eliminate $[A_i]$ matrices from the set of unknowns. Earlier MS developments enforced three approximation constraints to each $[\tilde{Q}]$ term in a way that eliminates $[A_0]$, $[A_1]$, and $[A_2]$. In this way the resulting least-square solutions in the $[D] \rightarrow [E] \rightarrow [D]$ iterations became of order n_a only, at the cost of increased error level. Because some approximation constraints are desired anyway, and because the increased approximation error was relatively small in many applications, the three-constraint approximation became a common practice. Reference 41, however, showed that the jth least-square problem in an unconstrained $[D] \rightarrow [E]$ iteration has the structure

$$\begin{bmatrix} C_{11} & 0 & C_{13} & C_{14} \\ 0 & C_{22} & 0 & C_{24} \\ C_{13} & 0 & C_{33} & C_{34} \\ C_{14}^T & C_{24}^T & C_{34}^T & C_{44} \end{bmatrix} \begin{Bmatrix} A_{0_j} \\ A_{1_j} \\ A_{2_j} \\ E_j \end{Bmatrix} = \begin{Bmatrix} b_1 \\ b_2 \\ b_3 \\ b_4 \end{Bmatrix} \tag{32}$$

where $[C_{11}]$, $[C_{22}]$, $[C_{13}]$, and $[C_{33}]$ are diagonal, and $[C_{44}]$ symmetric. This structure facilitates an efficient solution through a sequential reduction of the problem size, which is only slightly larger than the three-constraint solution.

A detailed description of the minimum-state procedure where the user can use any number of approximation constraints between 0 to 3 is given in Ref. 41. Several studies[25,26,40,41] compared the aeroelastic models resulting from the MS, Roger, and MMP approximations. The number of aerodynamic states, n_a, in the MS models were about 75% smaller than those of the Roger's models with similar accuracy, and 40–70% smaller than those of the MMP models. The additional computational cost because of the nonlinear nature of the MS rational approximation process is not severe because it is performed only at the database construction part of the basic optimization process, and is not involved in any sensitivity analysis (the modes are fixed). The number of aerodynamic states required for an adequate accuracy with the MS method in typical aeroservoelastic design models[14,28,42] is 4–10. A smaller number of states is required when the physical weighting technique of the next section is applied.

Physical Weighting

The physical-weighting algorithm developed in Refs. 26, 42, and 43 was designed to weigh each term of the tabulated data such that the magnitude of the weighted term indicates its relative importance in the aeroelastic solution. The idea is that the weight assigned to a data term should be proportional to the estimated effect of a unit approximation error on a representative aeroelastic property. Different representative properties were selected for the structural, control, and gust-related partitions of the AFC matrices. The error effects are estimated by the differentiation of the selected aeroelastic properties with respect to the aerodynamic terms. The weight calculations are performed with the coefficients of Eq. (17), with s replaced by ik_lV/b. The weighting dynamic pressure is $q = q_d$ at which the open-loop system is stable.

The weights assigned to the terms of a structure-related AFC matrix $[Q_{hh}(ik_l)]$ are based on their effect on the determinant of the system matrix $[C_s(s)]$ of Eq. (17) with $s = ik_l$. The partial derivatives of this determinant with respect to $Q_{hh_{ij}}(ik_l)$, divided by the determinant itself, is shown in Ref. 26 to be the absolute value of the (i, j) term of $[C_s(ik_l)]^{-1}$. Hence, the weight matrix associated with $[Q_{hh}(ik_l)]$ is

$$[\bar{W}_{hh}]_l = q_d \left| [C_s(ik_l)]^{-1} \right|^T \tag{33}$$

The weights assigned to the terms in the jth column of a control-related AFC matrix $[Q_c(ik_l)]$ is based on the open-loop Nyquist frequency response of the jth actuator to excitation by the jth control surface, with all other actuators locked. The actuator response is related to the modal response by

$$\{\delta_c(i\omega)\} = [T(i\omega)][\phi_{sh}]\{\xi_h(i\omega)\} \tag{34}$$

where $[T(i\omega)]$ is a matrix of transfer functions relating actuator outputs to sensor inputs. The transfer functions used for physical weighting should be simple and not necessarily related to particular aeroservoelastic parameters. Structural, narrow-band filters with high sensitivity to parametric changes should not be included as it may result in the assignment of low weights to important aerodynamic data terms. The jth Nyquist return signal is obtained by substituting $\{\xi_h(s)\}$ of Eq. (17), with $s = i\omega$ and with zero right-hand side except for the terms associated with ξ_{c_j}. The weights assigned to $Q_{hc_{ij}}(ik_l)$ is the magnitude of the partial derivative of the Nyquist signal with respect to $Q_{hc_{ij}}(ik_l)$, which is shown in Ref. 26 to be equal to the (i, j) term of the weight matrix

$$[\bar{W}_{hc}]_l = q \left| [T(ik_l)][\phi_{sh}][C_s(ik_l)]^{-1} \right|^T \tag{35}$$

The weights assigned to the terms of the gust column $\{Q_{hg}(ik_l)\}$ are based on the power spectral density (PSD) of the open-loop response of a selected structural acceleration to continuous gust, derived from Eq. (17):

$$\Phi_z(k_l) = |(k_l^2 qV/b^2)[\phi_{zh}][C_{hh}(ik_l)]^{-1}\{Q_{hg}(ik_l)\}|^2 \Phi_w(k_l) \quad (36)$$

where $[\phi_{zh}]$ is a row vector of modal displacements at the selected response point, and $\Phi_w(k)$ is the PSD function of the associated gust velocity. The weight assigned to $Q_{hg_l}(ik_l)$, is the partial derivative of $\sqrt{\Phi_z(k_l)}$ with respect to $Q_{hg_l}(ik_l)$, which yields the weight vector

$$\{\bar{W}_{hg}\}_l = (k_l^2 qV/b^2)|[\phi_{zh}][C_s(ik_l)]^{-1}|^T \sqrt{\Phi_w(k_l)} \quad (37)$$

The proposed physical weighting identifies the important generalized aerodynamic terms and their frequency range of particular importance. It might produce, however, extreme weight variations between terms. When applied in a single least-square solution, such weight variations have the effect of neglecting much of the data, which may cause numerical ill-conditioning problems and unrealistic curve fits. To ensure realistic interpolation between the tabulated k values, and to facilitate the application of the resulting aeroelastic model to a variety of flow conditions, structural modifications, and control parameters, it may be desirable to moderate the weight variations. This can be done by one or a combination of the following means: 1) assignment of relatively large damping parameters in $[B_{hh}]$ in Eq. (17), 2) widening the weight peaks, and 3) scaling up the extremely low weights. Various applications demonstrated that the resulting aeroservoelastic models were adequate for analyses with large variations of dynamic pressures,[26,41–43] control gains,[28,44] and structural parameters.[28,35]

Elimination of Structural States

The relative magnitude of a weighted aerodynamic term is a measure for its aeroelastic importance. When all of the weighted aerodynamic terms (over frequency) of a certain mode are small, the associated modal displacement and velocity can be eliminated from the vector of independent states by either truncation of residualization.[25,27] It is assumed at this point that the aeroservoelastic model of Eq. (24) has already been established with an initial set of vibration modes, and that it is now desired to reduce the model size by eliminating the structural states that have a negligible effect on the model accuracy. The state vector $\{x\}$ is partitioned into two subsets, $\{x_1\}$ and $\{x_2\}$, where $\{x_2\}$ is to be constrained and eliminated from the state vector, and $\{x_1\}$ is to be retained. In our case, $\{x_1\}$ includes all of the aerodynamic, control, and gust states, and the retained structural states, and $\{x_2\}$ includes only structural states $\{\xi_2\}$ and $\{\dot{\xi}_2\}$.

The state elimination is performed by partitioning Eq. (24) according to $\{x_1\}$ and $\{x_2\}$, using the bottom partition for eliminating $\{x_2\}$ as

$$\{x_2\} = [F]\{x_1\} + [G]\{u\} + \{G_w\}w + [H]\{\dot{x}_1\} \quad (38)$$

and then substituting Eq. (38) in the top petition of Eq. (24). The coefficients of Eq. (38) depend on the type of the state elimination procedure.

The simplest and most commonly used size-reduction technique is truncation. It is based on the assumption that the eliminated states have no effects on the dynamics and on the output of the system, namely the coefficient matrices of Eq. (38) are all zero. The resulting model is that of Eq. (24) where all the rows and columns associated with $\{x_2\}$ are truncated.

Static residualization assumes that the $\{\xi_2\}$ effects are important but the $\{\dot{\xi}_2\}$ and $\{\ddot{\xi}_2\}$ effects may be neglected. It can be shown[27]that the resulting $[G]$ and $\{G_w\}$ coefficients in Eq. (38) are zero, which means that the output part of Eq. (24) remains with no noise term and that its $\{y_s\}$ partition remains with no control term either. These features help in subsequent dynamic stability and response analyses. Also, as shown in Ref. 27, the matrix coefficients of the resulting state-space equation have the same topology (zero partitions) as those of the full-size equation [Eq. (24)]. The static residualization assumption is actually the one applied to all the elastic modes in the static aeroelastic equilibrium equation [Eq. (8)].

The dynamic residualization technique of Ref. 27 retains the effects of both $\{\xi_2\}$ and $\{\dot{\xi}_2\}$ on the retained states, but still neglects the effects of $\{\ddot{\xi}_2\}$. The resulting reduced-size model matrices do not keep their original topology and may have nonzero control and gust terms in the output equations. However, the accuracy of the reduced-size models may increase significantly. Reference 28 demonstrated a 10-step aeroservoelastic optimization case where 14 out of the 25 database modes were dynamically residualized with a negligible effect of the optimization results. The total number of states was reduced from 62 to 34, reducing the CPU time per optimization step by 75%. Because of the changed topology, Ref. 28 used the reduced-order models to calculate the stability and response constraints, but reverted to the full model for the sensitivity calculations. Reference 45 extended the residualization formulation to sensitivity analysis and demonstrated additional time savings. The extension facilitates efficient application of modern robust-control design methods that are based on sensitivities of the plant matrices.

Control System Model Assembly

The control system is modeled as an interconnection of three types of basic control elements in addition to the actuator element of Eq. (22). The element types are 1) single-input/single-output (SISO) s domain transfer function, 2) multi-input/multi-output (MIMO) subsystem given in the form of the state-space realization matrices of Eq. (21), and 3) zero-order junction (JNC) element. The interconnections among the control elements and between them and the aeroelastic plant can be either fixed or through variable gains. A schematic example of a control system, from sensor outputs to actuator inputs, is shown in Fig. 2. This structure facilitates efficient assembly, control margin calculations, and sensitivity analysis with respect to control design variables. A SISO element is to be used to represent analog filters, and a MIMO element typically represents a control subsystem defined in a separate design process. The G_i connections in Fig. 2 represent variable gains with respect to which control margins are calculated. The control margins used in aeroservoelastic design are either SISO gain and phase margins calculated with the gain connections opened one at a time, or MIMO margins in terms of singular values.[39]

The control elements of Fig. 2 are assembled in the database construction phase of the optimization process in the state-space form of Eq. (21). This assembly implements the fixed interconnections that are marked in Fig. 2 by the thick links. The G_i connections remain open in this realization. The control element arrangement is designed such that each control gain connects an output term $\{y_c\}$ with an input term $\{u\}$ in Eq. (21), which yields a diagonal $[G_c]$ in Eq. (25). For a given architecture of the control system, the individual elements in Fig. 2 can always be defined such that the control design variables p_{c_k} appear as control gains. The use of the variable gains as control design variables in the aeroservoelastic optimization process is very convenient because the associates sensitivity analysis is straightforward.[39,44]

Dynamic Stability and Response Considerations

The use of fixed-basis state-space aeroservoelastic models in optimization with dynamic stability and response considerations is detailed in Refs. 28, 44, and 46. The efficiency of the optimization process is obviously affected by the order n of the state-space model, with the CPU time proportional to n^2 to

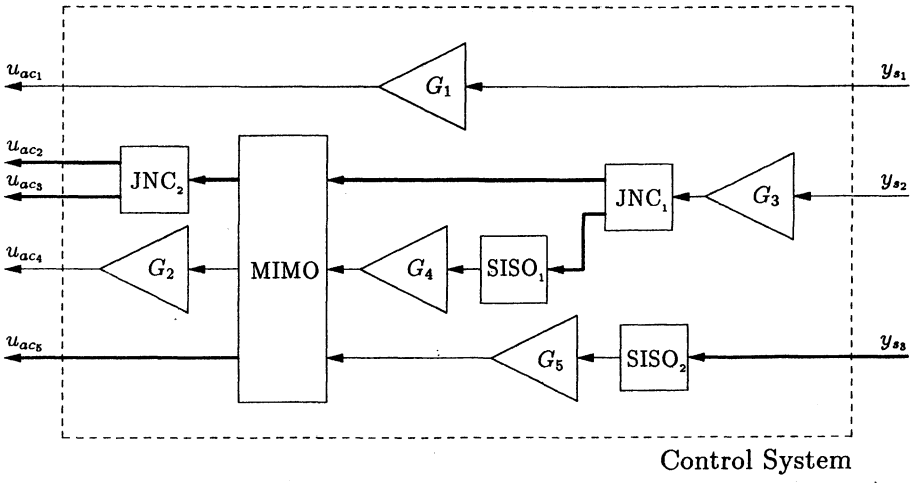

Fig. 2 Control system interconnection model.

n^3. Additional modeling issues that affect the optimization efficiency are discussed next.

The main ingredients for the sensitivity analysis of stability and response constraints are the derivatives of the state-space matrices of Eq. (26), which are based on the matrices of Eqs. (20–25). The use of a fixed modal basis implies that the structural design variables affect only the partitions that depend on the generalized structural matrices $[M_{hh}]$, $[M_{hc}]$, and $[K_{hh}]$. Such partitions appear in Eq. (20) and in the acceleration and stress outputs in Eq. (24). The linear dependence of the generalized matrices on the design variables, as in Eqs. (3) and (4), is usually adequate. The use of higher-order terms, such as in important bending effects where structural matrices depend on structural design variables in a nonlinear manner, does not add a significant difficulty.[46] As discussed in the previous section, the control design variables affect the closed-loop system matrix (26) only through the diagonal gain matrix $[G_c]$ in Eq. (25).

Dynamic response constraints to either deterministic[32] or continuous-gust[46] excitations may require special modeling considerations, as they should appear as outputs in $\{y_s\}$ of Eq. (24). The application of the motion and stress outputs discussed after Eq. (24) as optimization constraints might be too costly, particularly in time-response cases, because of the large number of parameters to be monitored and differentiated. A practical approach is to monitor integrated section load parameters, such as shear forces and bending moments, and to assure that they do not exceed previously defined loads envelopes.

The inclusion of integrated loads as outputs of Eq. (24) requires the definition of kinematic integration load modes $[\phi_{aL}]$. The integration can then be performed by either the MD or the SOF approaches. The extension of the dynamic loads formulation of Ref. 32 to our fixed-basis case yields the MD section loads

$$\{L_{\mathrm{MD}}(t)\} = [M_{Lh}][M_{hh}]^{-1}[K_{hh}]\{\xi_h(t)\} \tag{39}$$

where $[K_{hh}]$ and $[M_{hh}]$ are the updated generalized matrices of Eqs. (3) and (4), and $[M_{Lh}]$ is defined similarly to $[M_{hc}]$ in Eq. (4), with $[\phi_{aL}]$ replacing $[\phi_{ac}]$. The SOF section loads are calculated by

$$\{L_{\mathrm{SOF}}(t)\} = [\phi_{aL}]^T\{P_a(t)\} - [M_{Lh}]\{\ddot{\xi}_h(t)\} \tag{40}$$

where $\{P_a(t)\}$ is the external loads vector, including the unsteady aerodynamic loads. While the SOF expression is more accurate, it requires the inclusion of integrated aerodynamic matrices $[Q_{Lh}Q_{Lc}Q_{Lg}]$ in the rational approximation process. It can be done without increasing the model size and without affecting the coefficient matrices of Eq. (18), which are already defined for $[Q_{hh}Q_{hc}Q_{hg}]$. The already defined $[E]$ is used in a single $[E] \rightarrow [D]$ iteration, explained after Eq. (31), that calculates special loads-related $[A_0]$, $[A_1]$, $[A_2]$, and $[D]$ matrices. The use of the approximation matrices for including SOF loads in the outputs of Eq. (24) is detailed in Ref. 32.

Conclusions

A whole array of size-reduction techniques for the determination of efficient static and time-domain aeroservoelastic models were presented. With all of the techniques using a common set of 30–50 fixed generalized coordinates, aeroservoelastic optimization can be performed in a single very efficient integrated process. Fictitious masses can be used to facilitate an accurate account of local loads and large structural changes. Perturbation modes allow the inclusion of stress considerations in static maneuvers and dynamic response cases. The regular modal basis can be expanded to include static displacement modes calculated in previous optimization steps, which increases accuracy and accelerates convergence. Various rational function approximation methods for the unsteady aerodynamic force coefficients were reviewed with a common notation. Among those, the classic Roger's method is the easiest to apply, but its resulting number of aerodynamic states is typically larger than that of the MS method. With physical weighting of the aerodynamic data, the number of MS aerodynamic states is small relative to the number of structural states. The physical weights can also be used to rate the structural modes according to their relative aeroelastic importance. The less important modes can then be eliminated by either truncation, static residualization, or dynamic residualization. The control system was included in a very general way, which allows convenient interaction with other control synthesis processes, and easy inclusion of control design variables in the structural design process. The optimization algorithm was designed such that the relatively heavy computations are performed in a preliminary database creation run. Numerous design studies with different design cases, behavior constraints, side and move limits, and analysis options can then be performed in an efficient, on-line manner.

References

[1]Livne, L., "Integrated Multidisciplinary Aeroservoelastic Synthesis: Background, Progress, and Challenges," *Multidisciplinary Design Optimization: State-of-the-Art*, edited by N. Alexandrov and M. Y. Husseini, Society for Industrial and Applied Mathematics, 1995.

[2]Livne, E., "Integrated Aeroservoelastic Optimization: Status and Direction," AIAA Paper 97-1409, April 1997.

[3]Bisplinghoff, R. L., Ashley, H., and Halfman, R. L., *Aeroelasticity*, Addison–Wesley, Reading, MA, 1955.

[4]Bisplinghoff, R. L., and Ashley, H., *Principles of Aeroelasticity*, Wiley, New York, 1962.

[5]Neill, D. J., Johnson, E. H., and Confield, R., "ASTROS—A Multidisciplinary Automated Structural Design Tool," *Journal of Aircraft*, Vol. 27, No. 12, 1990, pp. 1021–1027.

[6]Climent, H., and Johnson, E. H., "Aeroelastic Optimization Using MSC/NASTRAN," *Proceedings of the International Forum on Aeroelasticity and Structural Dynamics* (Strasbourg, France), Association Aéronautique et Astronautique de France, Paris, 1993, pp. 1097–1116.

[7]Livne, E., Schmit, L. A., and Friedmann, P. P., "Integrated Structure/Control/Aerodynamic Synthesis of Actively Controlled Composite Wings," *Journal of Aircraft*, Vol. 30, No. 3, 1993, pp. 387–394.

[8]Giles, G. L., "Equivalent Plate Analysis of Aircraft Wing Box Structure with General Planform Geometry," *Journal of Aircraft*, Vol. 23, No. 11, 1986, pp. 859–864.

[9]Bindolino, G., Lanz, M., Mantegazza, P., and Ricci, S., "Integrated Structural Optimization in the Preliminary Aircraft Design," *Proceedings of the 17th Congress of the International Council of the Aeronautical Sciences* (Stockholm, Sweden), 1990, pp. 1366–1378.

[10]Noor, A. K., and Lowder, H. E., "Approximate Techniques of Structural Reanalysis," *Computers and Structures*, Vol. 4, No. 4, 1974, pp. 801–812.

[11]Sheena, Z., and Karpel, M., "Static Aeroelastic Analysis Using Aircraft Vibration Modes," *Proceedings of the 2nd International Symposium on Aeroelasticity and Structural Dynamics* (Aachen, Germany), Deutsch Gesellschaft für Luft- und Raumfahrt (DGLR), Bonn, Germany, 1985, pp. 229–232.

[12]Karpel, M., and Sheena, Z., "Structural Optimization for Aeroelastic Control Effectiveness," *Journal of Aircraft*, Vol. 26, No. 5, 1989, pp. 493–495.

[13]Huang, X., Haftka, R. T., Grossman, B., and Mason, W. H., "Comparison of Statistical Weight Equations with Structural Optimization of a High Speed Civil Transport," *Proceedings of the AIAA/USAF/NASA/ISSMO 5th Symposium on Multidisciplinary Analysis and Optimization* (Panama City, FL), AIAA, Washington, DC, 1994, pp. 1135–1144.

[14]Karpel, M., and Brainin, L., "Stress Considerations in Reduced-Size Aeroelastic Optimization," *AIAA Journal*, Vol. 33, No. 4, 1995, pp. 716–722.

[15]Karpel, M., Moulin, B., and Love, M. H., "Modal-Based Structural Optimization with Static Aeroelastic and Stress Constraints," *Journal of Aircraft*, Vol. 34, No. 3, 1997, pp. 433–440.

[16]Karpel, M., "Modal Based Enhancement of Integrated Structural Design Optimization Schemes," *Proceedings of the AIAA/NASA/ISSMO 6th Symposium on Multidisciplinary Analysis and Optimization* (Bellevue, WA), AIAA, Reston, VA, 1996, pp. 1223–1232.

[17]Moulin, B., and Karpel, M., "Static Condensation in Modal-Based Structural Optimization," *Structural Optimization*, Vol. 15, No. 3/4, Springer–Verlag, Berlin, 1998, pp. 275–283.

[18]Kirsch, U., "Reduced Basis Approximations of Structural Displacements for Optimal Design," *AIAA Journal*, Vol. 29, No. 10, 1991, pp. 1751–1758.

[19]Kirsch, U., "Improved Stiffness-Based First-Order Approximations for Structural Optimization," *AIAA Journal*, Vol. 33, No. 1, 1995, pp. 143–150.

[20]Karpel, M., and Raveh, D., "Fictitious Mass Element in Structural Dynamics," *AIAA Journal*, Vol. 34, No. 3, 1996, pp. 607–613.

[21]Haftka, R. T., and Yates, E. C., Jr., "Repetitive Flutter Calculations in Structural Design," *Journal of Aircraft*, Vol. 13, No. 6, 1976, pp. 454–461.

[22]Newsom, J. R., Able, I., and Dunn, H. J., "Application of Two Design Methods for Active Flutter Suppression and Wind-Tunnel Test Results," NASA TP-1653, April 1980.

[23]Mukhopadhyay, V., Newsome, J. R., and Abel, I., "A Method for Obtaining Reduced-Order Control Laws for High-Order Systems Using Optimization Techniques," NASA TP-1876, March 1981.

[24]Roger, K. L., "Airplane Math Modeling and Active Aeroelastic Control Design," AGARD, CP-228, 1977, pp. 1–11.

[25]Karpel, M., "Size-Reduction Techniques for the Determination of Efficient Aeroservoelastic Models," *Control and Dynamic Systems*, Vol. 54, Academic, San Diego, CA, 1992, pp. 263–295.

[26]Karpel, M., "Time Domain Aeroservoelastic Modeling Using Weighted Unsteady Aerodynamic Forces," *Journal of Guidance, Control, and Dynamics*, Vol. 13, No. 1, 1990, pp. 30–37.

[27]Karpel, M., "Reduced-Order Aeroelastic Models via Dynamic Residualization," *Journal of Aircraft*, Vol. 27, No. 5, 1990, pp. 449–455.

[28]Karpel, M., "Multidisciplinary Optimization of Aeroservoelastic Systems Using Reduced-Size Models," *Journal of Aircraft*, Vol. 29, No. 5, 1992, pp. 939–946.

[29]Mukhapedayay, V., "Control Law Synthesis and Stability Robustness Improvement Using Constrained Optimization Techniques," *Control and Dynamic Systems*, Vol. 32, Academic, San Diego, CA, 1990, pp. 163–205.

[30]Chen, P. C., Liu, D., Sarhaddi, D., Striz, A. G., Neill, D. J., and Karpel, M., "Enhancement of the Aeroservoelastic Capability in ASTROS," U.S. Air Force Wright Labs., TR-96-3119, Sept. 1996.

[31]Blakely, K., "MSC/NASTRAN Basic Dynamic Analysis," *User's Guide*, Vol. 68, MacNeal-Schwendler Corp., Los Angeles, CA, 1993.

[32]Karpel, M., and Presente, E., "Structural Dynamic Loads in Response to Impulsive Excitation," *Journal of Aircraft*, Vol. 32, No. 4, 1995, pp. 853–861.

[33]Livne, E., "Accurate Calculation of Control Augmented Structural Eigenvalue Sensitivities Using Reduced Order Models," *AIAA Journal*, Vol. 27, No. 7, 1989, pp. 947–954.

[34]Karpel, M., "Efficient Vibration Mode Analysis of Aircraft with Multiple External Store Configurations," *Journal of Aircraft*, Vol. 25, No. 8, 1988, pp. 747–751.

[35]Karpel, M., and Wieseman, C. D., "Modal Coordinates for Aeroelastic Analysis with Large Local Structural Variations," *Journal of Aircraft*, Vol. 31, No. 2, 1994, pp. 396–403.

[36]Rodden, W. P., and Love, R. L., "Equations of Motion of a Quasi-steady Flight Vehicle Utilizing Restrained Static Aeroelastic Characteristics," *Journal of Aircraft*, Vol. 22, No. 9, 1985, pp. 802–809.

[37]Karpel, M., Moulin, B., and Love, M. H., "Structural Optimization with Stress and Static Aeroelastic Constraints Using Expanded Modal Basis," AIAA Paper 98-1868, April 1998.

[38]Karpel, M., "Design for Active Flutter Suppression and Gust Alleviation Using State-Space Aeroelastic Modeling," *Journal of Aircraft*, Vol. 19, No. 3, 1982, pp. 221–227.

[39]Karpel, M., Idan, M., and Cohen, D., "Aeroservoelastic Interaction Between Aircraft Structural and Control Design Schemes," AIAA Paper 98-1864, April 1998.

[40]Tiffany, S. H., and Adams, W. M., Jr., "Nonlinear Programming Extensions to Rational Function Approximation Methods for Unsteady Aerodynamic Forces," NASA TP-2776, July 1988.

[41]Karpel, M., and Strul, E., "Minimum-State Unsteady Aerodynamic Approximations with Flexible Constraints," *Journal of Aircraft*, Vol. 33, No. 6, 1996, pp. 1190–1196.

[42]Karpel, M., and Hoadley, S. T., "Physically Weighted Approximations of Unsteady Aerodynamic Forces Using the Minimum-State Method," NASA TP-3025, March 1991.

[43]Karpel, M., "Extension to the Minimum-State Aeroelastic Modeling Method," *AIAA Journal*, Vol. 29, No. 11, 1991, pp. 2007–2009.

[44]Karpel, M., "Sensitivity Derivatives of Flutter Characteristics and Stability Margins for Aeroservoelastic Design," *Journal of Aircraft*, Vol. 27, No. 4, 1990, pp. 368–375.

[45]Herszberg, I., and Karpel, M., "Flutter Sensitivity Analysis Using Residualization for Actively Controlled Flight Vehicles," *Structural Optimization*, Vol. 12, No. 4, Springer–Verlag, Berlin, 1996, pp. 229–236.

[46]Zole, A., and Karpel, M., "Continuous Gust Response and Sensitivity Derivatives Using State-Space Models," *Journal of Aircraft*, Vol. 31, No. 5, 1994, pp. 1212–1214.